

Internal Report
DESY D3-42
May 1982

Eigentum der Property of	DESY	Bibliothek library
Zugang: Accessions:	1. JULI 1982	
Leihfrist: Loan period:	7	Tage days

Synchrotron Radiation in the PETRA Tunnel
for Beam Energies up to 30 GeV

H. Dinter

DESY behält sich alle Rechte für den Fall der Schutzrechtserteilung und für die wirtschaftliche Verwertung der in diesem Bericht enthaltenen Informationen vor.

DESY reserves all rights for commercial use of information included in this report, especially in case of filing application for or grant of patents.

**“Die Verantwortung für den Inhalt dieses
Internen Berichtes liegt ausschließlich beim Verfasser“**

SYNCHROTRON RADIATION IN THE PETRA TUNNEL FOR BEAM ENERGIES UP
TO 30 GEV

Internal Report DESY D3/42

May 1982

H.Dinter

ABSTRACT

The energy fractions of the synchrotron radiation absorbed by the components of a PETRA dipole magnet, and absorbed energy doses and spectra of the radiation escaping from a dipole magnet into the PETRA tunnel have been calculated for beam energies between 17 and 30 GeV.

CONTENTS

1.0 INTRODUCTION 1

2.0 CALCULATIONS 2

2.1 Absorbed Energy in a Dipole Magnet 2

2.2 Absorbed Energy Doses in the Tunnel 7

2.3 Photon Spectra in the Tunnel 13

3.0 CONCLUSIONS 13

LIST OF ILLUSTRATIONS

Figure 1.	The critical energies of PETRA, HERA and LEP	2
Figure 2.	PETRA dipole magnet	3
Figure 3.	Absorbed energy fractions	4
Figure 4.	Variation of the lead shielding	6
Figure 5.	Suggested dipole shielding for high beam energies	7
Figure 6.	Escaped energy fractions	8
Figure 7.	Geometry for dose calculations within the tunnel	10
Figure 8.	Absorbed energy doses in the tunnel along 3 lines	11
Figure 9.	Absorbed energy doses in the tunnel at 3 points	12
Figure 10.	Doses at constant RF-power	14
Figure 11.	Energy fraction spectra	15

1.0 INTRODUCTION

Some recent papers report results of measurements of the synchrotron radiation in the PETRA tunnel at 17 GeV beam energy and their comparison with calculations (ref.1,2,3). There it is shown that the Monte Carlo code EGS (ref.4) is well suited to predict absorbed doses even in a complicated geometrical arrangement of different materials as it is represented by a dipole magnet. We found an agreement between measurements and calculations within a factor of 2 to 3.

The maximum beam energy of PETRA will be increased in the near future. Therefore it is useful to have some informations about the increase of the absorbed energy in the dipole magnet components, and of the doses in the tunnel as well. The agreement at 17 GeV justifies predictions for higher energies up to 30 GeV.

In the following chapters results are given from calculations for two types of geometries:

1. An infinitely long dipole magnet (identical to the magnet in ref.2). The fraction of the incoming energy absorbed in the main components of the magnet are calculated.
2. A slightly simplified dipole magnet placed within the rectangular PETRA tunnel. The absorbed doses in the tunnel are calculated along three lines:
 - a horizontal line in beam height,
 - a vertical line near the gap of the magnet and
 - a vertical line below the yoke of the magnet.

In addition, the energy fraction spectra for one point of each line at a distance of appr. 50 cm from the beam are given.

All doses in the tunnel are expressed as absorbed doses in RPL-glass (radio-photoluminescence glass).

For more details concerning dosimetry and calculation methods see ref.2, 3 and 5.

NOTE: Radiation problems of different accelerators are similar at the same critical energy. Therefore in Figure 1 on page 2 the critical energies of the three big machines PETRA, HERA and LEP are compared for illustration.

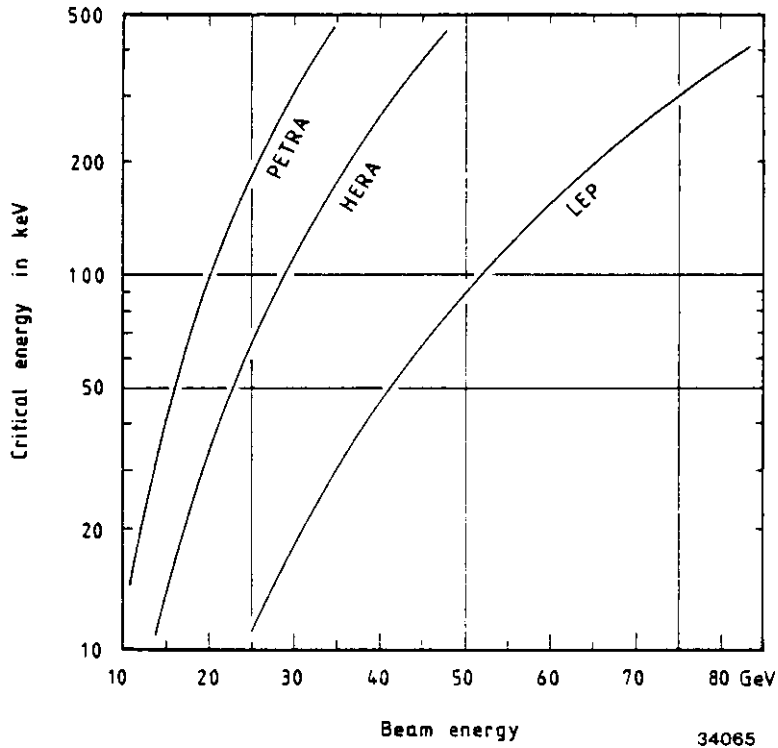


Figure 1. The critical energies of PETRA, HERA and LEP

2.0 CALCULATIONS

2.1 ABSORBED ENERGY IN A DIPOLE MAGNET

The arrangement of the magnet components used for the EGS input is a rectangular approach of a PETRA dipole (Figure 2 on page 3).

Each rectangle represents a region where the absorbed energy fraction is determined. Summing up the contributions of all regions belonging to one component the energy fractions plotted in Figure 3 on page 4 are obtained as a function of energy.

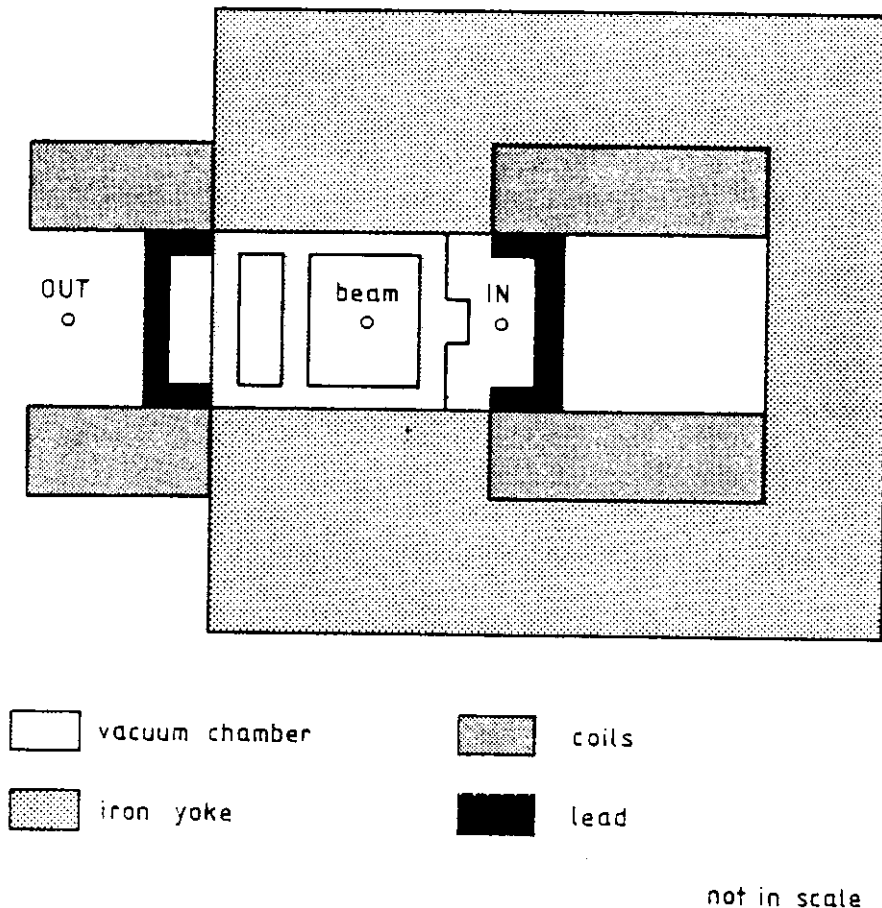


Figure 2. PETRA dipole magnet: Geometrical configuration used for the calculation. The energy spectra at the points OUT and IN are given in Figure 11 on page 15

The lead shield inside and outside the iron yoke is 3 mm as it is presently the case at PETRA.

Most fractions do not change very drastically up to 30 GeV, some of them are even constant at higher energies. Only the fraction of energy absorbed in the coils grow up to one order of magnitude between 17 and 30 GeV. The highest increase (1.5 orders of magnitude) shows the energy fraction escaping through the magnet gap into the tunnel. This part of the scattered synchrotron radiation determines the doses being present in the

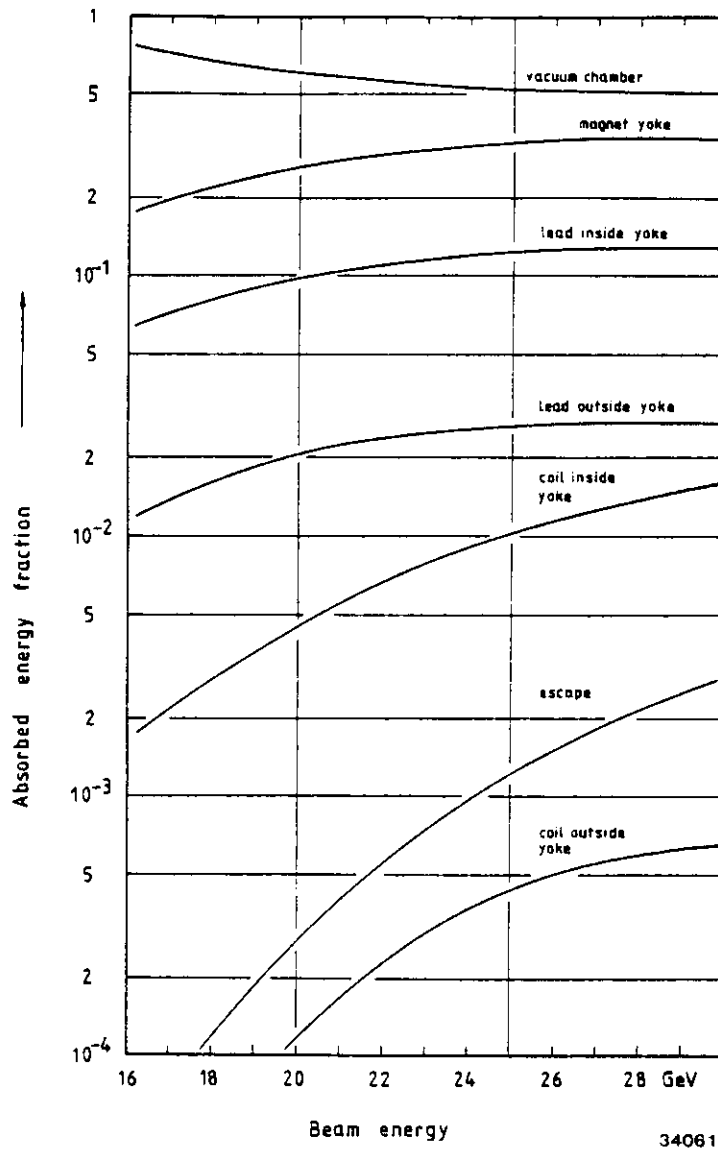


Figure 3. Absorbed energy fractions: Calculations for all components of the dipole magnet between 17 and 30 GeV. The vacuum pipe is shielded by 3 mm of lead inside and outside the magnet yoke.

tunnel (the magnet iron is an ideal shielding; almost no photons are able to penetrate it) and it is worthwhile to try to reduce it.

Therefore calculations were performed with a variety of lead thicknesses and arrangements.

To summarize the results of these calculations, the absorbed and escaped energy fractions are compared with those plotted in Figure 3 on page 4 which represent the present shielding status (3 mm of lead) and which are listed in Figure 4 on page 6.

The increase of both layers of lead (inside and outside the magnet) up to 10 mm do not influence the energy fractions (excepted a 20 %-effect at the inner coils), especially the escaped fraction remains constant. In fact, more photons are absorbed in the lead shield outside the yoke but this effect is compensated by a higher backscatter rate at the lead inside the magnet.

That means that a thick outer shield and a thin or no inner shield could lower considerably the escaped energy. Indeed, the calculations result in a 50 to 70 % reduction of the escaped energy fraction for 10 mm of lead outside and 3 mm of lead inside the magnet, while the absorbed energy in the inner coils does not change compared with the 3 mm inside/3 mm outside version.

The inner coils are critical components with respect to radiation damage. An improvement of the protection could be achieved by changing the inner lead shield as illustrated in Figure 5 on page 7.

As indicated in the last column of Figure 4 on page 6 the decrease of the absorbed energy fraction for the inner coils would be about 80 % by only 4 mm of lead at both surfaces of the coils whereas no change of the escaped energy is expected compared with the previous version of 10 and 3 mm of lead.

The energy fractions escaped into the tunnel at various shielding combinations as a function of the beam energy are shown in Figure 6 on page 8.

2.2 ABSORBED ENERGY DOSES IN THE TUNNEL

Due to the energy escaping the dipole magnets a certain radiation level is present all over the tunnel, causing damage in accelerator components and producing noxious gases. Therefore there is interest in the amount and in the distribution of the doses.

Components	Lead Configuration				
	6/6	10/10	6/3	10/3	10/0 *
Vacuum chamber	1.	1.	1.	1.	1.
Magnet yoke	1.	1.	1.	1.	0.8
Lead inside yoke	1.	1.	1.	1.	1.5
Lead outside yoke	1.	1.	1.	1.	1.
Coils inside yoke	1.0→0.8	1.0→0.7	1.	1.	0.1→0.3
Coils outside yoke	1.	1.	1.	1.	1.
Escaping **	1.	1.	0.5	0.5→0.3	0.5→0.3

The range of ratios (a→b) corresponds to the energy range 17 to 30 GeV.

The notation a/b in the lead configuration means:
thickness of lead outside the magnet = a mm
thickness of lead inside the magnet = b mm

* Different shielding arrangement;
see text and Figure 5 on page 7.

** See also Figure 6 on page 8.

Figure 4. Variation of the lead shielding: Ratio of the absorbed and escaped energy fractions of various lead configurations to the present shielding status (3/3 mm).

The dose distributions are calculated along 3 lines (Figure 7 on page 10):

- horizontally, from the surface of the vacuum chamber to the inner wall of the tunnel (line H);
- vertically, from beam height at 25 cm distance from the vacuum chamber to the floor of the tunnel (line V1) and
- vertically, from the bottom of the magnet iron to the floor (line V2).

The influence of straight sections to the radiation field is not taken into account. The lead shield inside and outside the magnet is supposed to be 3 mm each.

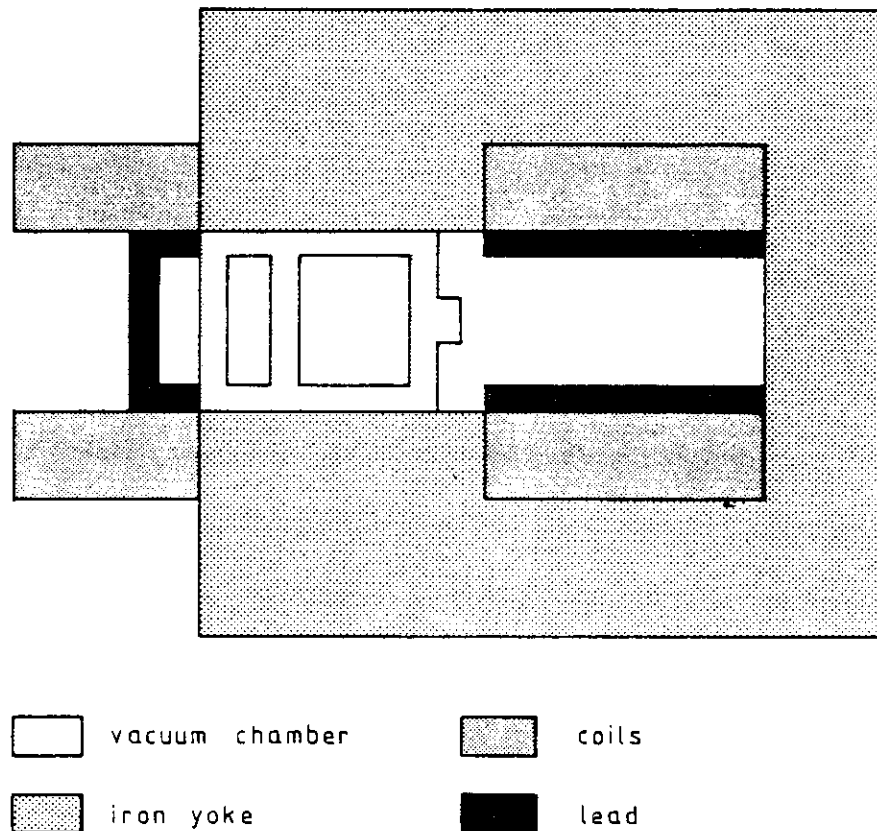


Figure 5. Suggested dipole shielding for high beam energies: a modification of the inner lead shield provides low escaping energy in connection with a good protection of the inner coils.

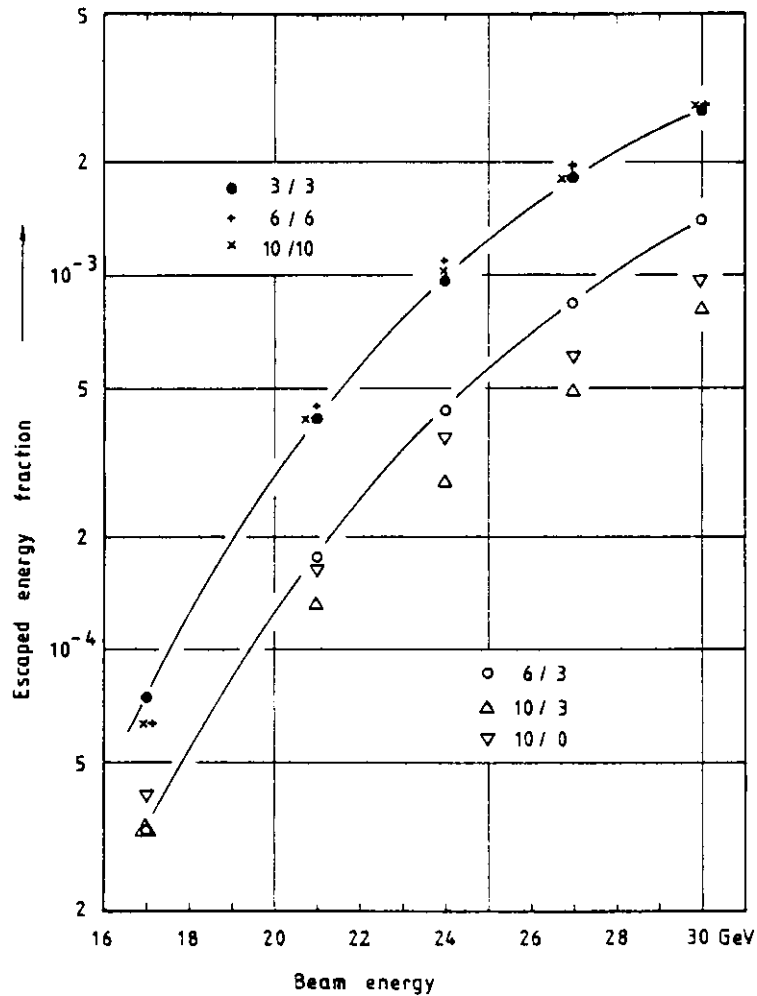


Figure 6. Escaped energy fractions: From a dipole magnet into the tunnel for some shielding configurations.

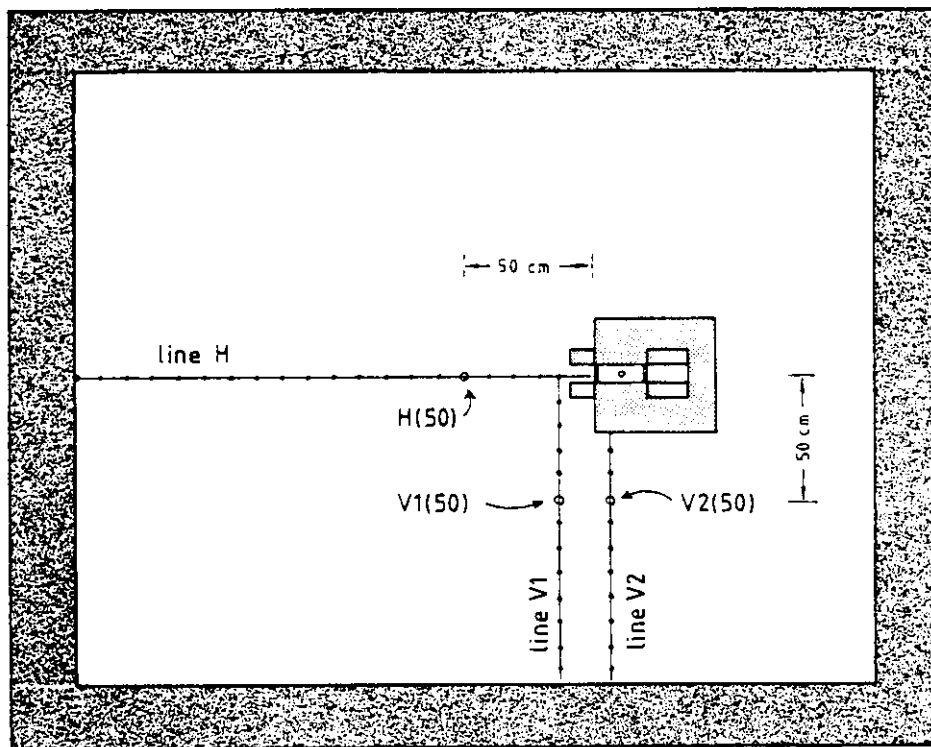
Notation a/b means:

a mm of lead outside the magnet and
b mm of lead inside the magnet

The configuration 10/0 refers to the lead arrangement shown in Figure 5 on page 7.

In Figure 8 on page 11 the calculated absorbed doses normalized to an integrated current of 0.1 Ah are plotted for 2 energies. The distance indicated on the abscissa for the graphs H is directed from the vacuum chamber horizontally to the wall, whereas for the graphs V it is directed vertically from beam height to the floor.

The radiation escapes the gap of the magnet with an azimuthal angular distribution depending on the beam energy. The doses at the beam level (along line H) are caused by photons which originate mostly from Compton scattering at the vacuum chamber or materials lying behind it. This source may be approximated by a line, and that is why we find a decrease of the horizontal doses going roughly with $1/r$.



34060

Figure 7. Geometry for dose calculations within the tunnel: The calculations were performed for points along the lines H, V1, V2. For the points H(50), V1(50), V2(50) energy spectra are given in Figure 11 on page 15.

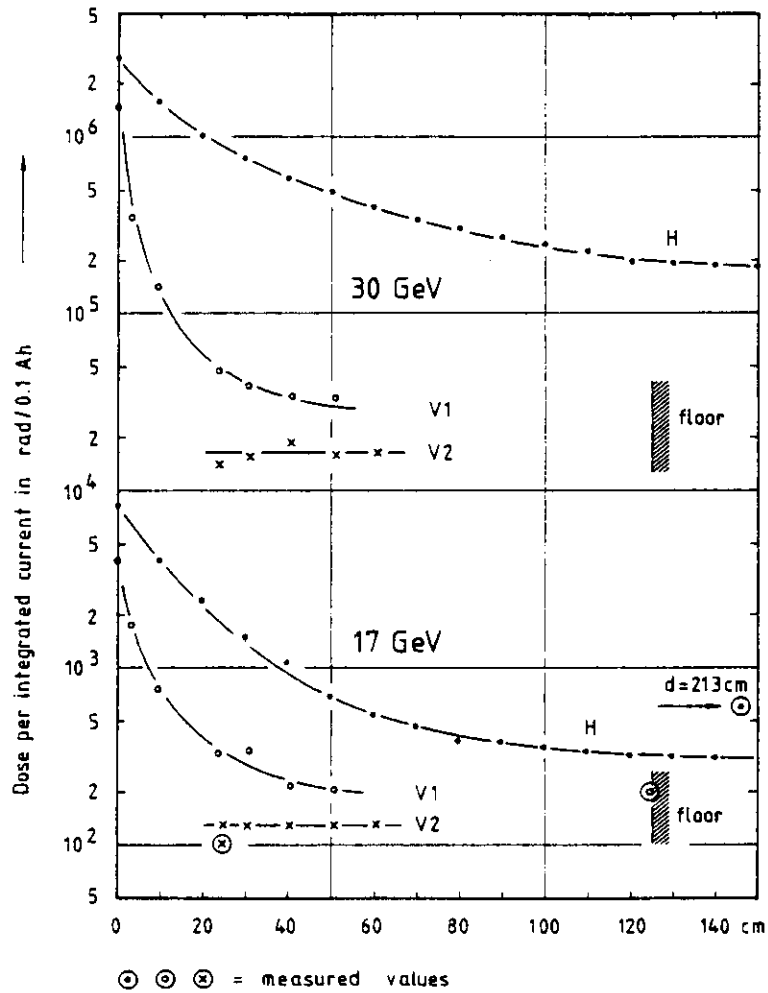


Figure 8. Absorbed energy doses in the tunnel along 3 lines: line H, line V1 and line V2 (see Figure 7 on page 10) for beam energies of 17 and 30 GeV. At 17 GeV three measured dose values are included. The lead shield is 3/3 mm.

Outside those regions which allow a view through the gap to the line source, the radiation level is dominated by photons scattered once or several times at the wall of the tunnel. Therefore curves V1, beginning at the high value of the horizontal plane, decrease rather quickly within the region where only multiply scattered tunnel background is present. This fact is confirmed by the curves V2 which do not receive any contribution from the line source directly. The doses below the magnet are constant and both curves V1 and V2 approach very close near the floor (which is difficult to calculate because of statistics).

As the angular distribution of Compton scattering depends on the energy the doses at high beam energies are more concentrated in the beam plane than at low energies. Therefore the difference between curves H and V increases with energy.

The graphs at 17 GeV in Figure 8 are provided with three points of measured absorbed doses (taken from ref. 1) which agree with the calculations within a factor of 2.

Most of the important components for the accelerator operation are installed within a distance of, say 50 cm from the beam pipe. Therefore the energy dependence of the doses at the corresponding points of the lines H and V are studied in more detail. The results are plotted in Figure 9 on page 12. While the doses at the points V1(50) and V2(50) increase with a constant ratio, the dose at H(50) rise much faster from a factor of 3 to a factor of 15 higher than V1(50).

The doses of Figure 8 and Figure 9 on page 12 are normalized to an accelerated electric charge of 0.1 Ah, an arbitrary values which equals to $2.25 \cdot 10^{21}$ particles. In order to estimate the finite life time of a component due to radiation damage one would prefer a normalization of the doses to a period of time and to a constant RF-power, rather than to an accelerated charge.

In Figure 10 on page 14 the doses of the curves of Figure 9 on page 12 are plotted with normalization to 1 MW of RF-power (pure accelerating power) and to 1 day. As an example it can be found that for an installed RF-power of 8 MW at 30 GeV and an average efficiency of, say 10 % (that means 0.8 MW of pure accelerating power) a daily dose of some 10^4 rad at 50 cm below the magnet are expected.

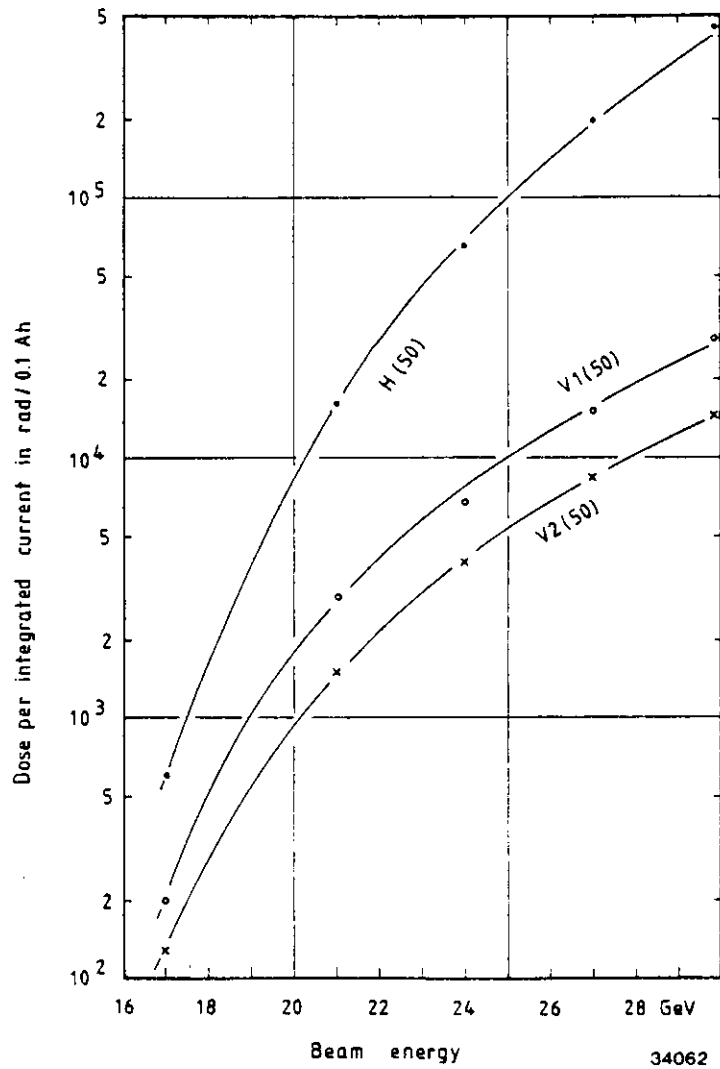


Figure 9. Absorbed energy doses in the tunnel at 3 points: at a distance of 50 cm from the beam pipe (geometry see Figure 7 on page 10) as a function of the beam energy (lead: 3/3 mm).

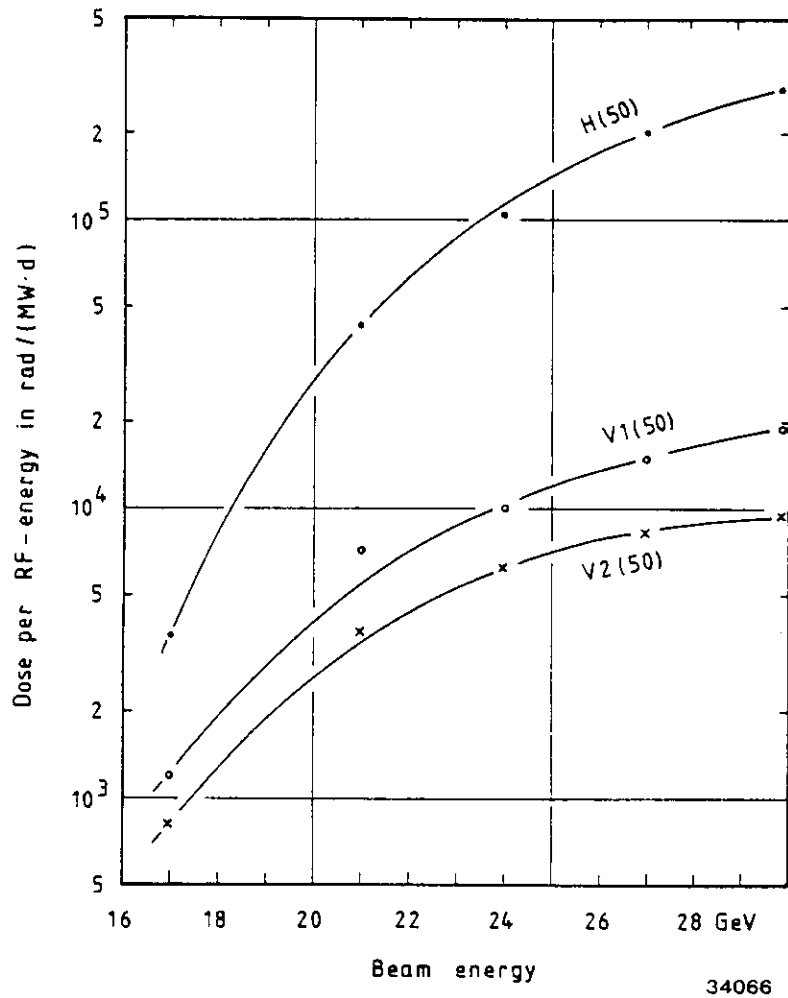


Figure 10. Doses at constant RF-power: For the points H(50), V1(50) and V2(50) the doses of Figure 9 on page 12 are displayed with a normalization to 1 MW and 1 day (lead: 3/3 mm).

2.3 PHOTON SPECTRA IN THE TUNNEL

For further reduction of the dose level in the tunnel by shielding, information about the spectral composition of the radiation field is necessary.

From the EGS code one obtains the energy flux entering a certain region of interest and its spectral distribution. Figure 11 on page 15 give the spectra of the energy fractions entering a $10 \times 10 \text{ cm}^2$ area around the point H(50), V1(50) and V2(50) (see Figure 7 on page 10) in addition to the spectra around the points "OUT" and "IN" (see Figure 2 on page 3) which are situated very near to the vacuum chamber outside (point OUT) and inside (point IN) the magnet.

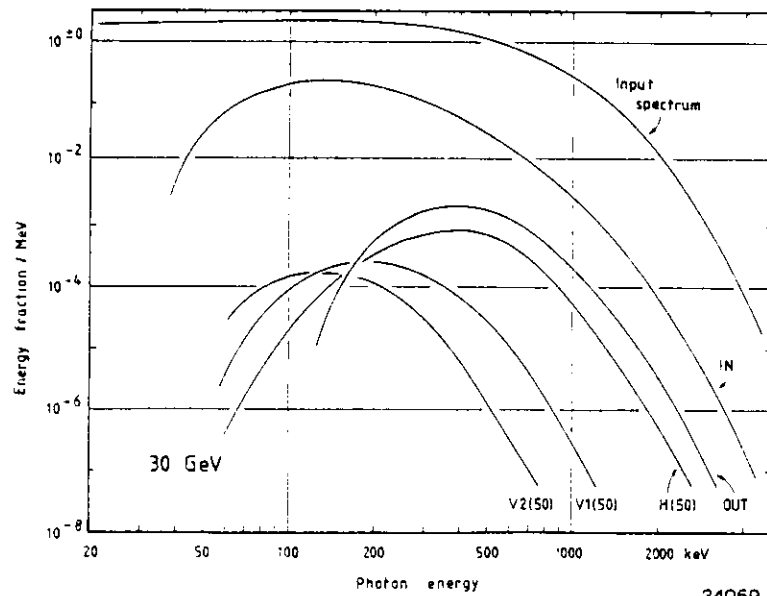
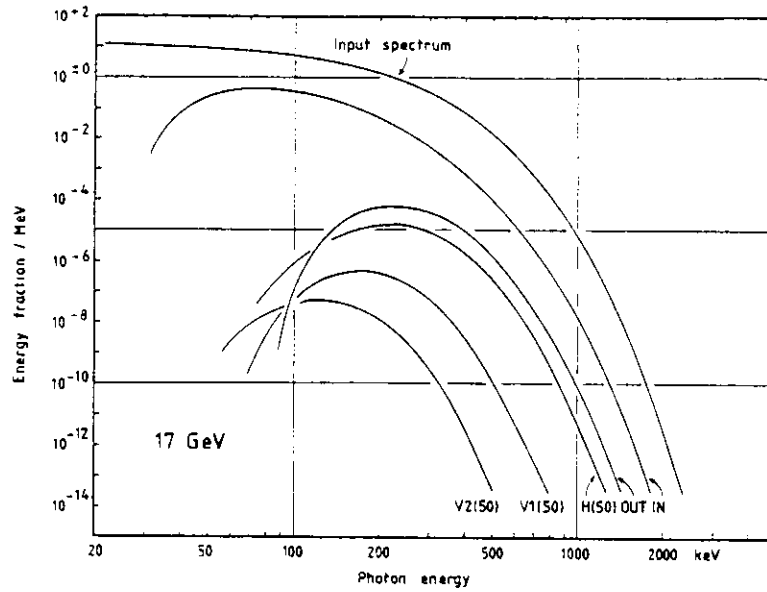
Comparing both sets of spectra at 17 and at 30 GeV one finds the expected enhancement of the photon intensities at high energies at 30 GeV and a clear shift of the spectrum maxima by a factor of 2 in energy at the points OUT, IN and H(50). In contrary to these points (where radiation originating from only one or a few scattering processes dominates) the maxima of the points V1(50) and V2(50) (where the multiply scattered background prevails) remain more or less constant.

The accuracy of the spectra suffers from poor statistics especially at low intensities, and the calculated values (not indicated in the drawing) fluctuate within one order of magnitude.

3.0 CONCLUSIONS

The fraction of energy absorbed in the dipole components in the present configuration do not change very much going up to 30 GeV. That means that even the absolute amount of dissipated energy in all components (except the coils) will remain approximately constant if the RF-power will be constant. The energy absorbed in the inner coils will increase by a factor of 20, unless measures are taken to improve the shielding arrangement as discussed in section 2.1. An increase by only a factor of 6 should be possible. However, it should be kept in mind that the calculated absorbed energy fractions have been obtained by summing over the whole component. Local effects at critical points have not been investigated. A more detailed study would be necessary.

The increase of the beam energy from 17 to 21 GeV in connection with the present RF-conditions roughly will increase the doses in the tunnel at a typical distance of 50 cm from the beam pipe by a factor of 10 in horizontal direction and by a factor of 5 in vertical direction.



34059

Figure 11. Energy fraction spectra:

Top: Beam energy 17 GeV

Bottom: Beam energy 30 GeV

Doubling the installed RF-power and increasing the beam energy to 24 GeV will result in an approximate increase by a factor of 60 horizontally and by a factor of 15 vertically for the points at 50 cm. A further increase to 30 GeV (again with doubled RF-power) will give a factor of around 150 higher doses at beam height, and a factor of around 30 higher doses below the dipole magnet.

Finally, a warning has to be added: Although the measurements verified the calculations at 17 GeV within a factor of 2, doses have been measured around the straight sections which are 3 to 5 times higher than the calculated doses due to imperfect shielding. If there are holes in the shielding (as it is actually the case), the doses may be even higher. The influences of straight sections and the associated bad shielding on the dose level in the tunnel is not included in the present calculations and demand for a certain safety factor.

REFERENCES

1. H.Dinter, K.Tesch: Some Measurements of Absorbed Dose Due to Synchrotron Radiation in th PETRA Tunnel.
Internal Report DESY D3/34, 1981
2. C.Yamaguchi: Absorbed Dose and Energy Deposition Calculation Due to Synchrotron Radiation from PETRA, HERA and LEP.
Internal Report DESY D3/38, 1981
3. H.Dinter, K.Tesch, C.Yamaguchi: Absorbed Dose Due to Synchrotron Radiation in the Storage Ring PETRA.
Nucl. Instr. and Methods, accepted for publication.
4. R.L.Ford, W.R.Nelson: The EGS Code System.
SLAC Report No. 210 (1978)
5. C.Yamaguchi: Comparison of Absorbed Dose to RPL Glass Dosimeter, Calculated by EGS Code, and Kerma.
Internal Report DESY D3/40, 1981 and Nucl. Instr. and Methods, accepted for publication.

